# REPORT DOCUMENTATION PAGE

AFRL-SR-BL-TR-98-

0645



| 1. AGENCY USE ONLY (Leave blank) | 2. REPORT DATE | 3. REPORT TYPE AND DATES COVERED |
|---|---|---|
| -- | 9/98 | Final Technical Report 6/95-5/98 |

**4. TITLE AND SUBTITLE**

GaAs-GaInP Superlattices for Intersubband Photodetection

**5. FUNDING NUMBERS**

F4960-95-1-0422

**6. AUTHOR(S)**

Dr. Manijeh Razeghi

**7. PERFORMING ORGANIZATION NAME(S) AND ADDRESS(ES)**

Northwestern University
Center for Quantum Devices
2225 N. Campus Drive, MLSB Room 4051
Evanston, IL 60208-3118

**8. PERFORMING ORGANIZATION REPORT NUMBER**

**9. SPONSORING/MONITORING AGENCY NAME(S) AND ADDRESS(ES)**

U.S. Air Force Office of Scientific Research/NE
110 Duncan Avenue
Suite B115
Bolling Air Force Base, DC 20332-6448

**10. SPONSORING/MONITORING AGENCY REPORT NUMBER**

**11. SUPPLEMENTARY NOTES**

**12a. DISTRIBUTION/AVAILABILITY STATEMENT**

**12b. DISTRIBUTION CODE**

**13. ABSTRACT** *(Maximum 200 words)*

We have demonstrated the first QWIP detectors using the quaternary InGaAlAs/InP materials system. We have observed excellent responsivity in the InGaAlAs/InP system compared to GaAs/AlGaAs QWIPs. By increasing the bandgap from ternary InGaAs to quaternary InGaAlAs we have shifted the responsivity out to longer wavelengths resulting in cutoff wavelengths of 13.3 and 19.4 μms, respectively for AlAs mole fractions of 0.1 and 0.15. We have also demonstrated lattice-matched mid-wavelength infrared detectors using InGaAs/InAlAs quantum wells. By combining both types of devices, we have produced the first lattice-matched dual band mid-wavelength and long-wavelength QWIP detectors on InP substrate. We have also demonstrated long-wavelength QWIPs ($\lambda$>12 μm) in GaAs-GaInP structures, and theoretically calculated the performance of these devices.

**14. SUBJECT TERMS**



**15. NUMBER OF PAGES**

**16. PRICE CODE**

| 17. SECURITY CLASSIFICATION OF REPORT | 18. SECURITY CLASSIFICATION OF THIS PAGE | 19. SECURITY CLASSIFICATION OF ABSTRACT | 20. LIMITATION OF ABSTRACT |
|---|---|---|---|
| | | | |

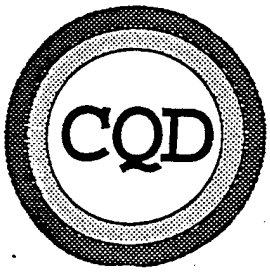


"GaAs-GaInP Superlattices for Intersubband Photodetection"

AFOSR Contract # F4960-95-1-0422 / NU #0650-350-S402
Project Manager: Dr. Gerald Witt

# FINAL TECHNICAL REPORT (AASERT)

**Principal Investigator:**

**Dr. Manijeh Razeghi**
**Center for Quantum Devices (CQD)**
**Northwestern University**

Outline

# Introduction

## Background

Infrared detection and thermal imaging are topics of strong interest for military programs, both for night vision and surveillance and also for weapon aiming. Alongside this is the rapid growth in the civil and commercial fields of applications of this technology which stretch from crime prevention to crop disease detection. For both military and civil applications, large staring arrays of infrared detectors provide the best spatial and temperature resolution images. This is reflected in the numerous theoretical and experimental studies of materials for use as detectors in infrared arrays that have steadily advanced the performance of these imaging systems.

The most challenging detectors to manufacture are those which are sensitive to infrared radiation at wavelengths greater than eight microns. The need for these long-wavelength infrared (LWIR) detectors derives from the fact that the infrared energy density radiated from objects at ambient temperatures reaches a maximum in the 8-14 micron region.

At present, advances in microelectronic fabrication and semiconductor crystal growth technology has allowed new physical phenomenon based on quantum mechanics to be used for infrared detection. Very thin semiconductor layers called quantum wells are used to construct quantum well infrared photodetectors (QWIPs) operating in the LWIR. Although at present they require lower operating temperatures to achieve the same sensitivity as other infrared sensors, QWIPs have several advantages including better uniformity, better large array manufacturability, and lower manufacturing costs.

The efforts of this AASERT were to provide a better experimental data base for a variety of new QWIP materials systems based on quantum wells and barriers made from $Ga_xIn_{1-x}As_yP_{1-y}$. materials. Currently, there is limited knowledge about QWIPs based on materials other than $GaAs/Al_xGa_{1-x}As$. New QWIP designs intended to improve sensitivity, especially designs developed to achieve multi-color, necessitate the use of these new quantum well materials. Thus the results of these studies will have direct technological significance by providing experimental growth, characterization, fabrication guidelines as well as a basic understanding of detector performance for these new materials.

## Objectives

General:

- High uniformity, background limited, multi-color detector arrays (focal plane arrays) operating in the infrared (IR) region between 3 and 20 μm.

Specific:

- Explore the use of GaAs and InP-based materials such as GaInP, InGaAs, InAlAs, InGaAsP, and InGaAlAs in quantum well infrared photodetectors (QWIP) designs and demonstrate improved performance by comparison to AlGaAs-GaAs QWIPs over the IR range 3 μm > λ > 20 μm.
- Develop very-long wavelength (λ>20 μm) QWIP detectors with better performance than mercury cadmium telluride (HgCdTe) detectors and higher temperature operation than cooled extrinsic detectors.
- Develop multi-color detectors lattice-matched to InP or GaAs with each pixel simultaneously sensitive to light in three IR wavelength bands: MWIR 3-5 μm, LWIR 8-12 μm and VLWIR : 12-20 μm.

## Applications

| | |
|---|---|
| Defense applications: | Night vision, camouflage countermeasures, land mine detection, reconnaissance, and space-base imaging. |
| Civilian applications: | Industrial manufacturing inspection, search and rescue and firefighting, medical imaging. |

## Major Achievements

### *For InP-based QWIPs:*

- Record-high responsivity > 8 A/W at $T$=77K for InGaAs/InP QWIPs.
- First experimental measurements of bias-dependant gain, quantum well capture probability, and recombination rate for InP-based QWIPs.
- Lower recombination rate results in higher detectivity, which allows higher temperature operation for LWIR detectors.
- 50X higher gain for InGaAs/InP vs. AlGaAs/GaAs indicates improved transport and carrier lifetime are obtained in InP-based materials.
- InGaAs/InAlAs 3-5 μm MWIR QWIPs demonstrate responsivity to 250K and record narrow FWHM of 0.13 μm.
- First demonstration of InGaAlAs/InP 8-20 μm LWIR QWIPs.
- First demonstration of two-color ( MWIR and LWIR ) QWIP detector lattice-matched to InP substrate.

### *For GaAs-based QWIPs:*

- Fabrication of QWIPs with peak responsivity at very long wavelengths, $\lambda_c \sim 15$ μm.
- Improved performance levels to $D^* = 3 \times 10^8$ at $T$=77K, quantum efficiency. ~ 14 %.
- Completed first theoretical modeling of GaAs-GaInP QWIPs. I-V curves; drift velocity, mobility carrier lifetime calculated from this model.
- Deliverables: First QWIP focal plane array in GaAs/GaInP demonstrated, and delivered to NASA-Goddard for testing.

### *Publications supported by this AASERT Grant*


1. C. Jelen, S. Slivken, M. Razeghi, "InGaAlAs/InP quantum well infrared photodetectors for 8-20 μm wavelengths," to be published in IEEE J. Quant. Electron., vol. 37 (1998).
2. C. Jelen, S. Slivken, T. David, M. Razeghi, "Noise performance of InGaAs/InP quantum well infrared photodetectors," IEEE J. Quant. Electron., vol. 34, pp. 1124-1128 (1998).
3. C. Jelen, S. Slivken, T. David, G.J. Brown, M. Razeghi, "Responsivity and noise performance of InGaAs/InP quantum well infrared photodetectors," Proc. SPIE vol. **3287**, pp. 12-21 (1997).
4. C. Jelen, S. Slivken, J. Hoff, M. Razeghi, "Aluminum–free GaInP/GaAs quantum well infrared photodetectors for long wavelength detection," Appl. Phys. Lett. **70**, pp. 360-362 (1997).
5. C. Jelen, S. Slivken, G. Brown, M. Razeghi, "GaAs/GaInP Quantum well intersubband photodetectors for focal plane array infrared imaging," Mat. Res. Soc. Symp. Proc. **450**, pp. 195-199 (1997).
6. C. Jelen, S. Slivken, G. Brown, M. Razeghi, "Very long wavelength GaAs/GaInP Quantum Well Infrared Photodetectors," Proc. SPIE vol. **2999**, pp. 144-152 (1997).
7. M. Tadic, C. Jelen, S. Slivken, M. Razeghi, "Photoresponse of InGaAsP-based p-doped quantum well infrared photodetectors," Proceedings of the IEEE International Conference on Microelectronics, v. 1, pp. 315-318, (1997).
8. M. Razeghi, C. Jelen, S. Slivken, J. Hoff "III-V interband and intraband far-infrared detectors," Inst. Phys. Conf. Ser. No. **155**, pp. 405-410. (1997).
9. J. Hoff, C. Jelen, S. Slivken, G. Brown, M. Razeghi, "Optical absorption and photoresponse in fully Quaternary p-type Quantum well detectors," Proc. SPIE vol. **2685**, pp. 62-71. (1996).
10. J. Hoff, C. Jelen, S. Slivken, E. Bigan, M. Razeghi, "Analysis of spectral response in p-type GaAs/GaInP QWIPs," Superlatt. & Microstruct. vol **18**, pp. 249-257 (1995).

# InP-Based QWIP Results

## *I. Background*

For some applications, MQW detectors lattice-matched to InP substrates have several advantages in comparison to LWIR MQW detectors composed of GaAs/$Al_xGa_{1-x}As$:

(1) The effective mass of electrons, which governs the drift mobility and tunneling properties, amounts to $0.042 \cdot m_o$ in $In_{0.53}Ga_{0.47}As$/InP compared to $0.067 \cdot m_o$ GaAs/AlGaAs, where $m_o$ is the free-electron mass;

(2) Mid-wavelength infrared (MWIR) 3-5 μm $In_{0.53}Ga_{0.47}As/Al_{0.48}In_{0.52}As$ quantum well detectors are lattice-matched with LWIR $In_{0.53}Ga_{0.47}As$/InP QWIP detectors, allowing a 2-color MWIR-LWIR lattice-matched detector stack to be grown on InP. This minimum intersubband absorption wavelength that can be achieved in GaAs/AlGaAs QWIPs is 6 μm. [1]

Since the photoresponse spectrum of an $In_{0.53}Ga_{0.47}As$/InP QWIP has a maximum at approximately 8 μm, [6-9] the use of $In_xGa_{1-x}As_yP_{1-y}$ quantum wells has been studied [2] to allow longer wavelength ($\lambda \sim 12$ μm) detection. Because the InGaAlAs material system covers approximately the same bandgap energies as InGaAsP, it is interesting to compare the hot electron transport and performance of quantum well infrared photodetectors fabricated from these two materials.

The bandgap of InGaAlAs can be engineered between the two boundary ternary alloys, $In_{0.53}Ga_{0.47}As$ (0.76 eV) and $In_{0.52}Al_{0.48}As$ (1.46 eV). The growth of InGaAlAs alloy is relatively easier than InGaAsP due to the following reasons [3]: (1) only one group V element (As) is incorporated, avoiding the problem of As/P ratio control; (2) composition of the layer is controlled by each constituent element's flux intensity; and (3) near-unity sticking coefficients of the three group III elements facilitate reproducibility of composition.

## *II. Device Design*

For this experiment, six structures were grown by gas-source molecular beam epitaxy with arsine and phosphine as group V sources, elemental gallium and indium as group III sources, and elemental silicon as an *n*-type dopant source. The AlAs mole fraction in $In_{0.52}(Ga_{1-x}Al_x)_{0.47}As$ and the quantum well width for the three long-wavelength samples were ($x$=0, 56 Å), ($x$=0.1, 60 Å), and ($x$=0.15, 65 Å) respectively. Each structure consisted of twenty periods of InGaAlAs quantum wells separated by 400 Å InP barriers. Two mid-wavelength samples of $In_{0.53}Ga_{0.47}As/In_{0.52}Al_{0.48}As$ were grown with quantum well widths of 35 and 40 Å. Each structure consisted of twenty periods of $In_{0.53}Ga_{0.47}As$ quantum wells separated by 400 Å $In_{0.53}Al_{0.48}As$ barriers. Lastly, a multi-color structure consisted of 20 periods of $In_{0.53}Ga_{0.47}As$/InP (well width = 58 Å, barrier width =500 Å) and 20 periods of $In_{0.53}Ga_{0.47}As/In_{0.52}Al_{0.48}As$ (well width = 35 Å, barrier width = 400 Å). The quantum wells for all devices were doped $n$=$8 \times 10^{17}$ $cm^{-3}$. Top and bottom 0.6 μm layers of $n$=$1 \times 10^{18}$ $cm^{-3}$ $In_{0.53}Ga_{0.47}As$ were grown for ohmic contacts. Arrays of 400 $\mu m^2$ mesas were etched in a Plasma-Therm 770 ECR/RIE etch system. A mix of $H_2/Ar/Cl_2/CH_4$ gases was used. Finally, AuGe/Ni/Au ohmic contacts were evaporated onto the top and bottom contact layers.

## *III. Long-Wavelength Infrared Detector*

The relative responsivity spectra for these three samples were collected using a Mattson Galaxy 3000 FTIR. The responsivity spectrum of the three samples measured at $T$=10K are shown in Fig. 1. For a bias of -1 V (mesa top negative), the 50% long wavelength cutoff wavelengths for the three samples were 8.5, 13.3, and 19.4 μm, respectively. The spectral response was unchanged for all three samples in the temperature range from $T$=10K up to $T$=77K.

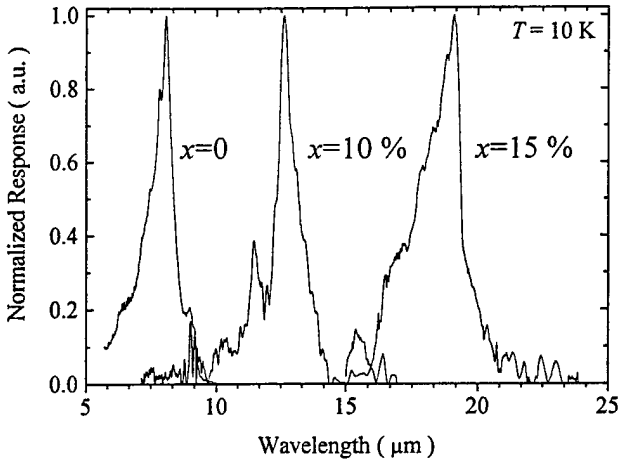


Fig. 1. Normalized spectral response for the three $In_{0.52}(Ga_{1-x}Al_x)_{0.48}As/InP$ QWIPs with $x$=0, $x$=0.1, and $x$=0.15 mole fraction of AlAs.

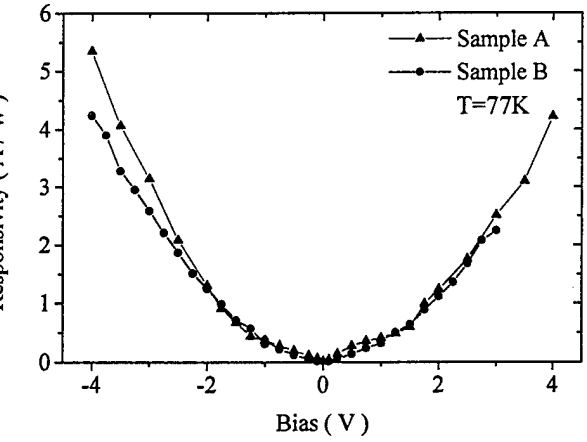


Fig. 2. Bias dependence of peak responsivity measured at $T$=77K for $In_{0.53}Ga_{0.47}As/InP$ and $In_{0.52}Ga_{0.38}Al_{0.1}As/InP$ QWIPs. No response was observed for the $In_{0.52}Ga_{0.33}Al_{0.15}As/InP$ QWIP at $T$=77K.

The absolute responsivities were measured by using a calibrated blackbody source. The detectors were back illuminated through a 45 ° polished facet. The bias dependence of the responsivity was measured for samples A and B at $T$=77K and the results are shown in Fig. 3 for both positive and negative bias. The responsivity of sample C was too low to be measured at $T$=77K. The peak responsivity at –1 V of the $In_{0.52}Ga_{0.38}Al_{0.1}As/InP$ QWIP (sample B) was 0.37 A/W. This is comparable (20 % higher) to the InGaAsP/InP QWIP (1.3 μm bandgap, $L_W$=63 Å) reported by Gunapala *et al.* [2] which had a similar 13.2 μm cutoff wavelength. It is worth noting the responsivity for these samples are approximately five times as large as the best responsivity measured for GaAs/AlGaAs QWIPs.

The noise current $i_n$, of the $In_{0.52}Ga_{0.38}Al_{0.1}As/InP$ and $In_{0.53}Ga_{0.47}As/InP$ QWIPs were measured at $T$=77K as a function of bias voltage using a spectrum analyzer and found to be $i_n$=23– and 0.3-pA at bias voltages of $V_B$= -0.5 V. The peak detectivities, $D^*_\lambda$ can now be calculated from $D^*_\lambda = R\sqrt{A\Delta f}/i_n$ where A=1.6×10$^{-4}$ cm$^2$ is the device area and $\Delta f$=1 Hz is the bandwidth. At an operating bias of $V_B$= -0.5 V and $T$=77K the measured values for the $In_{0.52}Ga_{0.38}Al_{0.1}As/InP$ QWIP are $R_P$=0.16 A/W, $i_n$= 23 pA/√Hz and thus D*=3x10$^8$ cm √Hz W$^{-1}$. The detectivity of the first sample (GaInAs/InP QWIP) at $T$=77K and $V_B$= -0.5 V is D* = 3.5x10$^{10}$ cm √Hz W$^{-1}$.

Using the spectral response data obtained for these samples, it is possible to estimate the conduction band offset for the $In_xGa_{1-x-y}Al_yAs/InP$ heterojunction. The cutoff wavelength for samples A, B, and C correspond approximately to the energy separation $\Delta E=E_2-E_1$ for the three aluminum compositions, y=0 (A), y=0.1 (B), and y=0.15 (C). The energies of the first and second allowed states for these InGaAlAs-InP samples can be calculated for several possible conduction band offsets using the well widths given in part II. The $E_g$ of $In_{0.52}(Ga_{1-x}Al_x)_{0.48}As$ layers was reported by Fujii *et al.* [4], and changes linearly from 0.75 eV to 1.47 eV with increasing $x$. The electron effective mass ($m_e$) of $In_{0.52}(Ga_{1-x}Al_x)_{0.48}As$ layers was reported by Olego et al. [5], and changes linearly from 0.041 to 0.075 with increasing $x$. A plot of the fit conduction band offset as a function of aluminum fraction is shown in Fig. 3. The

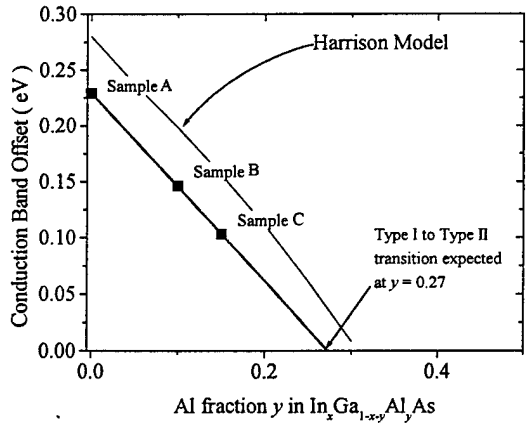


Fig. 3. Conduction band offset values from samples as a function of Al fraction $y$ in $In_xGa_{1-x-y}Al_yAs$. Also shown is a theoretically derived curve by Ishikawa [10].

data from samples A, B, and C are indicated on the figure. The line is the band offset predicted by the Harrison model as applied by Ishikawa *et al.* [6-7].

From the experimental data for these QWIPs, it would be expected that the transition from type I quantum well to type II staggered quantum well for $In_{0.53}(Ga_xAl_{1-x})_{0.47}As/InP$ heterojunctions would occur at $y$=0.27. This is less the value ($y$=0.33) predicted by the experimental model, which is based on an interpolation from binary data for InAs, GaAs, and AlAs, but larger than other recent experimental results for GSMBE-grown material: $y$=0.18 calculated from interband absorption by Kawamura, *et al.* [8], and $y$=0.23 calculated from Shottky diode dark currents by Chua *et al.* [3]. Because intersubband absorption is very sensitive to the conduction band offset, the measurements presented here represent an accurate method for determining this type I-to-type II transition composition.

## IV. Mid-Wavelength Infrared Detector

The responsivity spectrum of the two mid-wave samples measured at $T$=77K are shown in Fig. 4. For a bias of -1 V (mesa top negative), the 50% long wavelength cutoff wavelengths for the three samples were 4.05 and 4.32 μm, respectively. The absolute responsivity saturated at –4 V bias for both samples, with a peak value of ~ 35 mA/ W. The magnitude of the responsivity did not vary with temperature in the range $T$=77K to $T$=200K, as shown in Fig. 5. The maximum detectivity obtained at $T$=77K for these samples was ~ $1x10^{12}$ cm $\sqrt{Hz}$ $W^{-1}$.

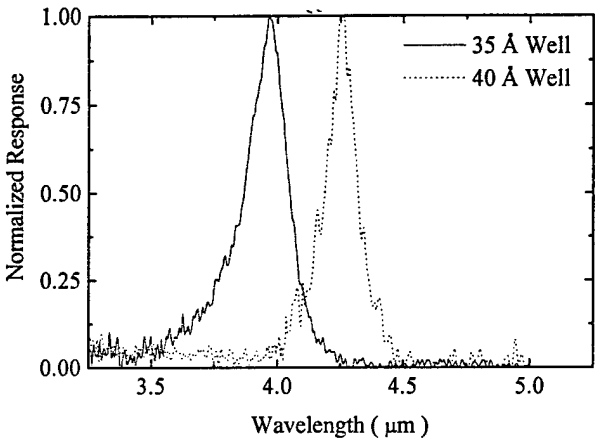


Fig. 4. Spectral response for $In_{0.53}Ga_{0.47}As/In_{0.52}Al_{0.48}As$ QWIPs for well widths of 35 and 40 Å.

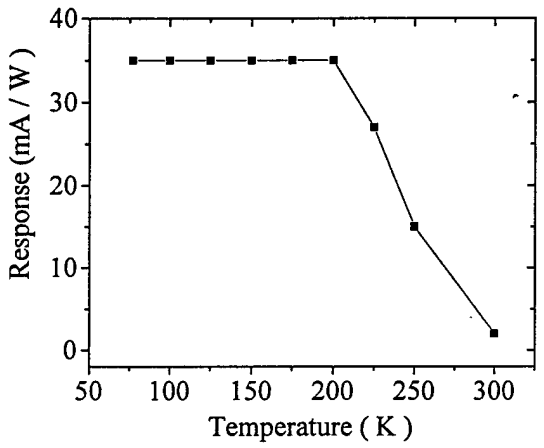


Fig. 5. Temperature dependence of peak responsivity for the 40 Å InGaAs/InAlAs QWIP sample.

## V. Dual Band Infrared Detector

A sample was grown for multispectral absorption in both MWIR and LWIR regions by including multiple quantum wells of both InGaAs/InAlAs and InGaAs/InP. Because the mask utilized in this work allows only one contact to be made to the mesa, the two MQW detectors are placed in series. At low biases, the electric field is applied mostly across the lower-resistance InGaAs/InP MQW. At higher biases, the electric field is applied across both MQWs, but the InGaAs/InP MQW is under such high field that no response is observed. Most carriers in the ground state tunnel out before absorption occurs, resulting in low LWIR photoresponse. A schematic of the processed device is shown in Fig. 6. The spectral response of this dual-band detector is shown in Fig. 7. for several biases. For biases less than 10V, the photoresponse in the 3-5 μm region is too noisy to resolve. For biases greater than ~ 7 volts, the photoresponse in the 8-9 μm region is no longer observed.

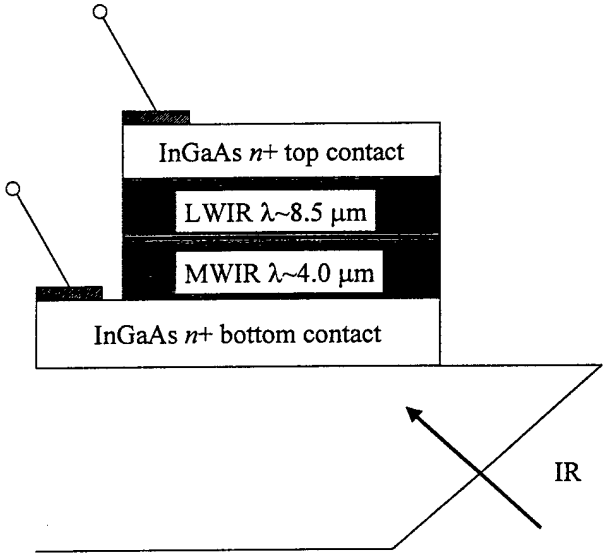


Fig. 6. Schematic diagram of a processed two-color detector.

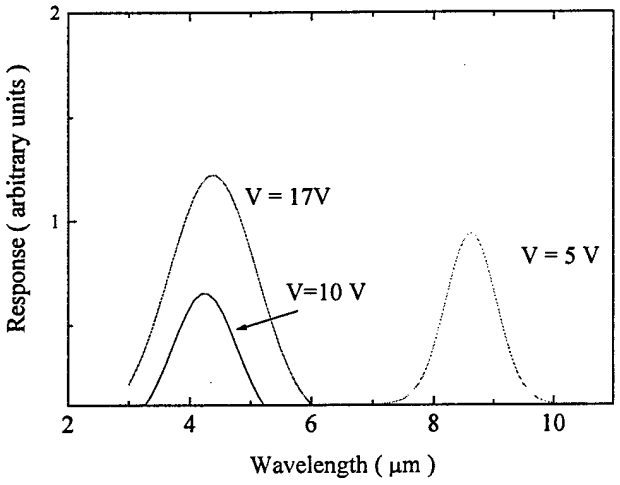


Fig. 7. Voltage dependence of the spectral response for the two-color detector, measured at $T$=77K.

## GaAs-Based QWIP Results

### *I. Structure.*

GaAs-GaInP n-type QWIP structures were grown using gas-source molecular beam epitaxy (GSMBE) on (100) semi-insulating GaAs substrates. GaAs well widths were 40Å, 65Å, and 75Å respectively, and the lattice-matched $Ga_{051}In_{0.49}P$ barriers were 500Å thick. Each sample superlattice had 20 periods. The silicon doping in the quantum wells was 5 x $10^{17}$ $cm^{-3}$.

### *II. Responsivity.*

The photoresponse for three different well widths is shown in Fig. 8. The peak wavelengths of the three samples are 10.4, 12.78, and 13.3 μm for well widths of 40, 67, and 75 Å respectively. The cutoff wavelengths are 13.5 μm, 15, and 15.5 μm for the three samples. The full width at half maximum (FWHM) for the three samples in meV (and as $\Delta\lambda/\lambda$) were 185 meV (0.58), 37 meV (0.5), and 42 meV (0.375) respectively. These FWHM are typical for bound to continuum QWIPs. The reduction in FWHM for wider wells indicates that the second excited state in these samples is closer to resonance with the barrier energy.

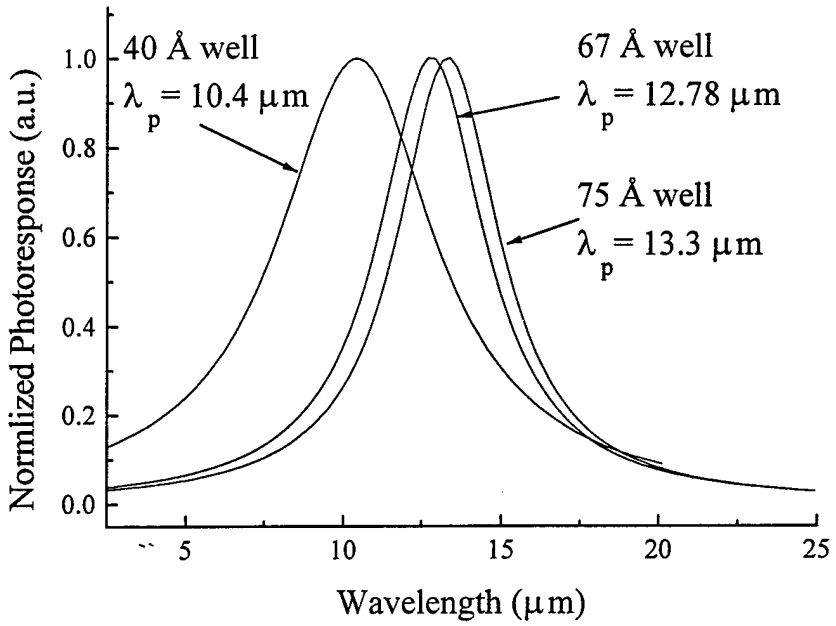


Fig. 8. Normalized optical response at 77K for samples with 40Å, 65Å and 75Å quantum wells.

Shown in Fig. 9 is the calculated absorption coefficient for a 75Å well GaAs/GaInP QWIP. The calculated peak absorption of 12.9 μm and an approximately 14 μm cutoff wavelength agree very well with the observed photoresponse shape.

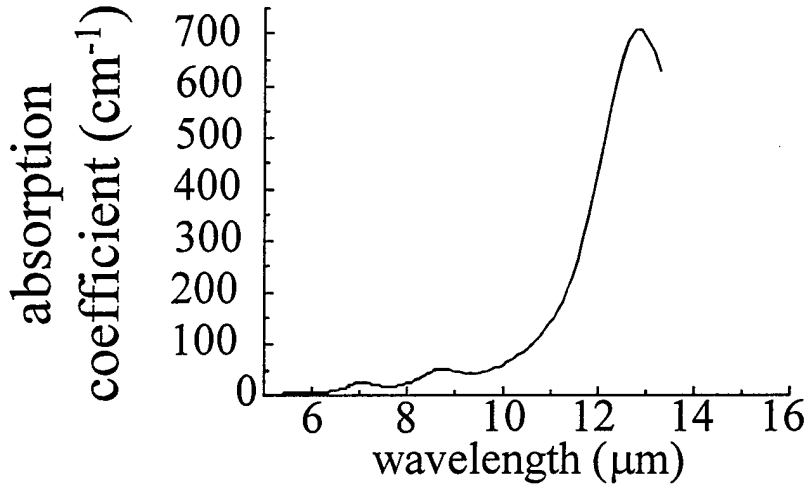


Fig. 9. Calculated absorption spectrum for 75Å GaAs / 500Å GaInP superlattice.

## *III. Dark Current.*

Figure 10 shows the typical dark currents measured at different temperatures. The observed asymmetry with bias may be due to an asymmetric quantum well profile or doping impurity segregation.

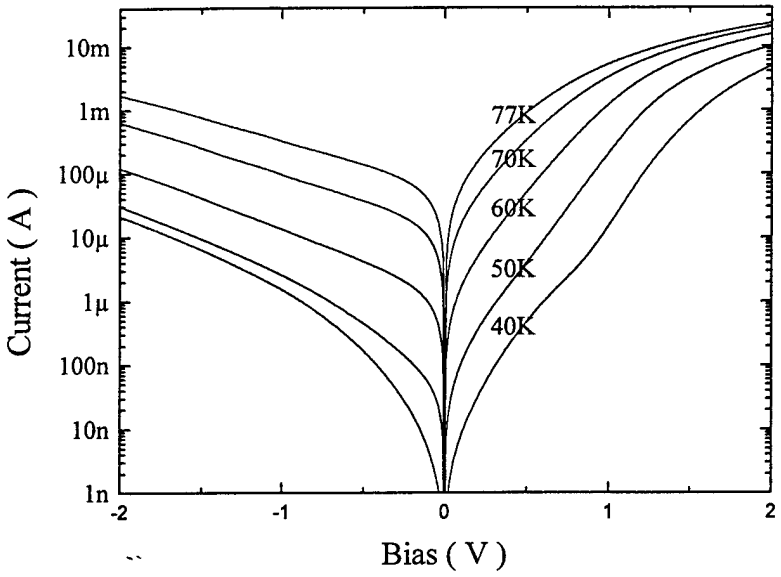


Fig. 10. Measured QWIP dark current from 30 to 77 K for the sample with 65 Å quantum wells.

At low bias, where tunneling can be neglected, the dark current $I$ is expected to increase exponentially with temperature following equation (1):

$$I \propto T \exp\left(-\frac{\Delta E}{kT}\right) \qquad \{1\}$$

Therefore, the activation energy can be obtained by calculating the slope of log ($I$/T) versus 1/kT. For the three samples with 40Å, 65Å, and 75Å wells, the activation energies ΔE are 37, 50, and 46 meV respectively.

The quantum well subband energies were determined using a four-band Kane model, which includes the effects of band non-parabolicity and band mixing. The electron-electron exchange interaction effect was also included, and the depolarization and excition shifts were neglected as before.

From these subband energy levels and the dark current activation energies we computed the conduction band offset $\Delta E_c$ to be 121.1 meV ± 2 meV. A summary of the data used in this model is given in Table I. From the known bad gaps of GaAs and GaInP, the band-gap difference $\Delta E_g$ = 483 meV is obtained[18]. Using our experimentally determined conduction band offset, a band ratio offset ratio of $\Delta E_c / \Delta E_g$ = 0.251 is calculated, which matches the assumed ratio used for theoretical modelling. Values of $\Delta E_c$ in the literature range between 80[19] to 240[5] meV. However, the only previous measurement for material grown by GSMBE was 108 meV[20]. This experimental result agrees well with these previous results.

TABLE I.

THE CONDUCTION BAND OFFSET IS CALCULATED AS $\Delta E_C = ( E_O - E_{EXCH} ) + E_F + \Delta E$, WHERE $E_O$ IS THE GROUND STATE, $E_{EXCH}$ IS THE ELECTRON-ELECTRON INTERACTION ENERGY, $E_F$ IS THE FERMI ENERGY, AND ΔE IS THE ACTIVATION ENERGY.

| Well (Å) | $E_o - E_{EXCH}$ | ΔE | $E_F$ | $\Delta E_c$ |
|---|---|---|---|---|
| 40 | 79 | 37 | 4.4 | 120.4 |
| 65 | 62 | 50 | 10.4 | 122.4 |
| 75 | 59 | 46 | 12.5 | 120.5 |

## *IV. Modeling*

A. DARK CURRENT

*1. Comparison to GaAs/AlGaAs*:

The dark current density ($A/cm^2$) at 77K for the 65Å sample as a function of electric field (V/cm) is shown in Figure 11. The results of Levine [1] for a GaAs/AlGaAs QWIP with similar well doping density, and cutoff wavelength is shown for comparison. The smaller dark current may be due to $GaAs/Ga_xIn_{1-x}P$'s larger mobility [9], smaller surface recombination velocity [10], or smaller interface roughness [11] by comparison to $GaAs/Al_xGa_{1-x}As$.

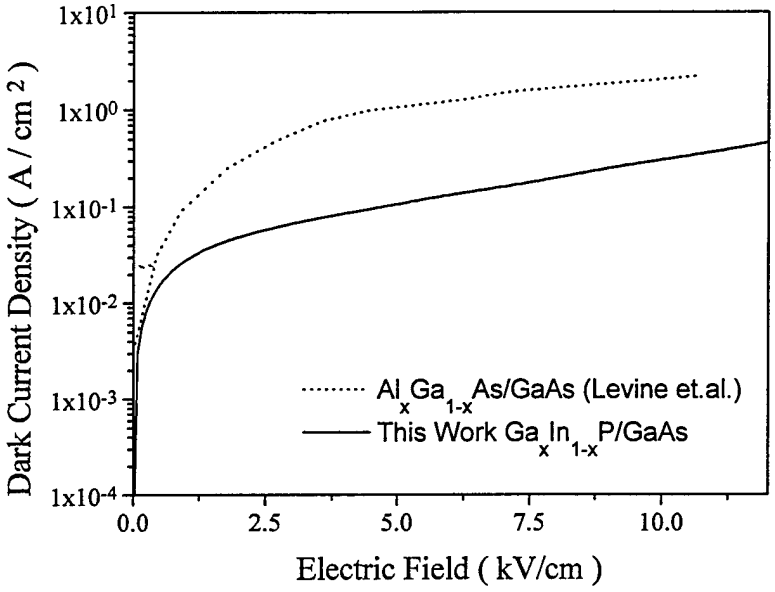


**Figure 11** Measured dark current density for sample C compared to GaAs/AlGaAs results in reference **[Error! Bookmark not defined.]**.

*2) Modeling:*

We have modeled the dark current by assuming thermodynamic carrier equilibrium and a drift model [12] where the drift velocity is proportional to the electric field according to:

$$v_d = \frac{\mu V}{L_b}\left[1+\left(\frac{\mu V}{v_s L_p}\right)^2\right]^{-1/2} \qquad \{2\}$$

where $\mu$ is the mobility, V is the applied bias per quantum well, and $L_p$ is the period thickness. We have neglected any complications to do with the way in which carriers in the quantum well are replenished and the mechanisms of charge transfer from the emitter contact to the MQW. Since the carriers which are thermally excited into the continuum transport states and contribute to the dark current are originally from the quantum wells, a 2-D density of states (DOS) is used. The effective number of carriers contributing to the current is then:

$$n = \left(\frac{m^*}{\pi\cdot\hbar^2}\cdot\frac{1}{L_p}\right)\int_{E_o}^{\infty} f_o(E)T(E,V)dE\,, \qquad \{3\}$$

where the term $m^*/\pi\hbar^2$ is the 2-D DOS, $f_o$(E,T) is the Fermi-Dirac distribution function, T(E,V) is the probability of tunneling through a a single barrier, and $E_o$ is the bound state energy (measured from the bottom of the band). In

this equation, the reason why the 2-D DOS is divided by the period width is to match the units, i.e. to convert sheet concentration into an average volumetric concentration. The dark current density is calculated using equation:

$$J = nev_d \qquad \{4\}$$

In calculating the transmission coefficient T(E,V) we have used T(E,V)=1 for E larger than the conduction band offset $V_o$ and the Wentzel-Kramers-Brillouin (WKB) approximation [13] for E< $V_o$. In the calculation we take the conduction band offset $V_o$ to be 0.1 eV. Conduction band non-parabolicity is neglected because it has been shown to have a negligible effect on dark current [14], but image charge effects have been included.

The dark current measurements for the 65Å sample are shown in Fig. 12 as function of voltage and temperature and compared with those calculated by equation {4}. Good agreement is achieved as a function of both bias and temperature over seven orders of magnitude in dark current. These calculations use a drift mobility of 1000 $cm^2\ V^{-1}\ s^{-1}$, a saturation velocity of 1.5 x $10^5$ $cm^{-1}$ and the nominal sample parameters shown in Table I. The saturation velocity is approximately one order of magnitude lower than typical values for bulk GaInP at 77K [15,16] in a similar electric field, as would be expected because of re-trapping by quantum wells and interface scattering.

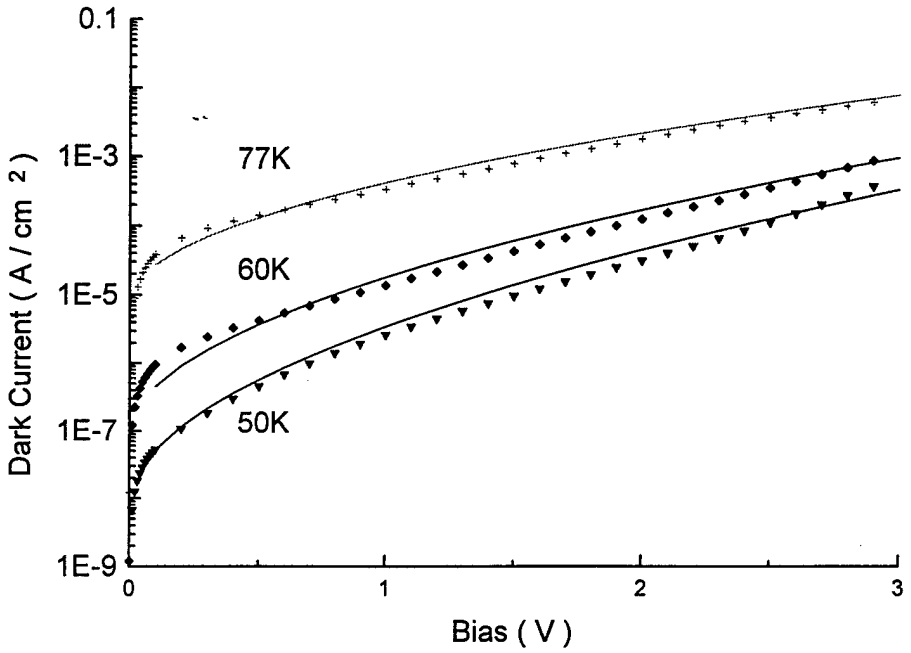


**Figure 12** Comparison of experimental (points) and theoretical (lines) dark current-voltage curves at various temperatures for sample B.

The photoconductive gain is ratio of the distance traveled by an electron before recapture *l* to the thickness of the device *L*. At the biases used in this experiment, $l = v_d(E)\cdot\tau$ and therefore

$$g = v_d(E)\cdot\tau / L. \qquad \{4\}$$

In order to evaluate the carrier lifetimes in these GaAs/GaInP detectors, we have directly measured the noise current as a function of bias using a spectrum analyzer at T=77K. This noise is dominated by generation-recombination noise at *T*=77K. From the equation for G-R noise given by $I_N=(4e\cdot I_d\cdot g)^{0.5}$, we calculate the gain using the dark current-bias data from Fig. 10, and then calculate the carrier lifetimes using equation {4}. Figure 13 shows the carrier lifetimes and gain derived from noise measurements for the 65Å sample.

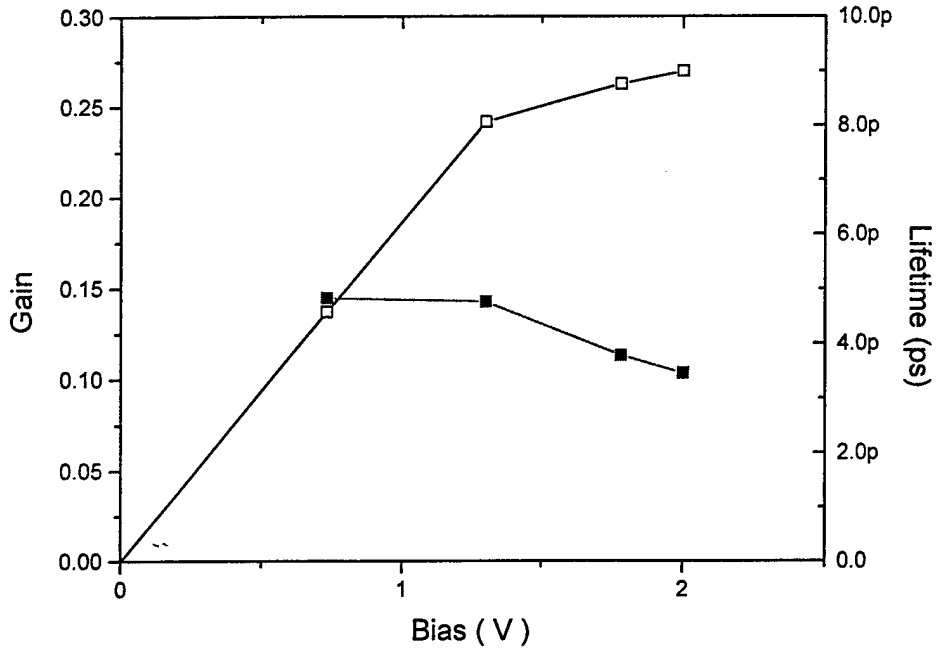


**Figure 13.** Calculated gain and recombination lifetimes as a function of applied bias for sample B.

## Conclusion

We have demonstrated the first QWIP detectors using the quaternary InGaAlAs/InP materials system. We have observed excellent responsivity in the InGaAlAs/InP system compared to GaAs/AlGaAs QWIPs. By increasing the bandgap from ternary InGaAs to quaternary InGaAlAs we have shifted the responsivity out to longer wavelengths resulting in cutoff wavelengths of 13.3 and 19.4 μms, respectively for AlAs mole fractions of 0.1 and 0.15. We have also demonstrated lattice-matched mid-wavelength infrared detectors using InGaAs/InAlAs quantum wells. By combining both types of devices, we have produced the first lattice-matched dual band mid-wavelength and long-wavelength QWIP detectors on InP substrate. We have also demonstrated long-wavelength QWIPs ($\lambda$>12 μm) in GaAs-GaInP structures, and theoretically calculated the performance of these devices.

## References


[1] B. Levine, "Quantum well infrared photodetectors," *J. Appl. Phys.* vol. **74**, No. 8, R1-R68, Oct. 1994.

[2] S.D. Gunapala, B.F. Levine, D. Ritter, R.A. Hamm, and M.B. Panish, "Lattice-matched InGaAsP/InP long-wavelength quantum well infrared photodetectors," *Appl. Phys. Lett.* vol. **60**, No. 5, pp. 636-638, Mar. 1992.

[3] S.J. Chua and A. Ramam, *Proceedings of the 1996 IEEE International Conference on Semiconductor Electronics, ISDE.* Piscataway, NJ: SPIE Press. pp.469-471, 1994.

[4] T. Fujii, Y. Nakata, Y. Sugiyama, and S. Hiyamizu, "MBE growth of InGaAlAs lattice-matched to InP by pulsed molecular beam method," *Jpn. J. Appl. Phys.* vol. **25 Pt.2: Letters**, No. 3, L254-L256 (1986).

[5] D. Olego, T.Y. Chang, E. Silberg, E.A. Caridi and A. Pinkzuk, "Compositional dependance of band-gap energy and conduction band effective mass of $In_{1-x-y}Ga_xAl_yAs$ lattice-matched to InP," *Appl. Phys. Lett.* vol. **41**, No. 5, pp. 476-478, Mar. 1982.

[6] T. Ishikawa and J.E. Bowers, "Band lineup and in-plane effective mass of InGaAsP or InGaAlAs on InP strained-layer quantum well," *IEEE J. Quant. Electron.* vol. **30**, No. 2, pp. 562-570, Feb. 1994.

[7] W.A. Harrison, "Elementary theory of heterojunctions," *J. Vac. Sci. Technol.* vol. **14**, No. 4, pp. 1016-1021, July/Aug. 1977.

[8] Y.Kawamura, H. Kobayahsi, and H. Iwamura, "Type I / Type II transition in InGaAlAs/InP multiple quantum well structures grown by gas-source molecular beam epitaxy," *Jpn. J. Appl. Phys.* vol. **33 Pt. 2: Letters**, No. 1B, pp. L79-L82, Feb. 1994.

[9] M. Razeghi, M. Defour, F. Ohmnes, M. Dobers, J. Vieren, Y. Guldner, "Extremely high electron mobility in a GaAs/GaInP heterostucture grown by metalorganic chemical vapor deposition," *Appl.Phys.Lett.* **55**, 457 (1989).

[10] J.M. Olson, R.K. Ahrenkiel, D.J. Dunlavy, B. Keyes, and A.E. Kibbler, "Ultralow recombination velocity at GaInP/GaAs heterointerfaces," *Appl.Phys.Lett.* **55**, 1208 (1989).

[11] W.C. Mitchel, G.J. Brown, K. Lo, S. Elhamri, M. Ahoujja, K. Ravindran, R. Newrock, X. He, M. Razeghi, "Interface roughness scattering in thin, undoped GaInP/GaAs quantum wells," *Appl.Phys.Lett.* **65**, 1578 (1994).

[12] S. Andrews and B. Miller, "Experimental and theoretical studies of the performance of quantum well infrared photodetectors," J.Appl.Phys. **70**, 993 (1991).

[13] R.H.Dicke and J.P.Wittke, *Introduction to Quantum Mechanics.* London, UK: Addison-Wiley (1960).

[14] S. Andrews and B. Miller, "Experimental and theoretical studies of the performance of quantum well infrared photodetectors," J.Appl.Phys. **70**, 993 (1991).

[15] K.F. Brennan, P. Chiang, "Calculated electron and hole steady-state drift velocities in lattice matched GaInP and AlGaInP," *J. Appl. Phys.* **71**, 1055 (1992).

[16] W.Masselink, N.Braslau, D.La Tulipe, W.Wang, and S.Wright, "Electron velocity at high electric fields in AlGaAs/GaAs modulation doped heterostructures," *Solid-State Electron.* **31**, 337 (1988).